Structural Engineering and Mechanics, Vol. 39, No. 2 (2011) 287-301 287
DOI: http://dx.doi.org/10.12989/sem.2011.39.2.287

Pressure impulse diagrams for simply-supported steel columns based on residual load-carrying capacities

Jong Yil Park*[1] and Theodor Krauthammer[2a]

[1]Agency for Defense Development, Joint Modeling and Simulation Center, PO Box 35-5 Yuseong, Daejon 305-600, Korea
[2]Center for Infrastructure Protection and Physical Security (CIPPS), University of Florida, 365 Weil Hall, PO Box 116580, Gainesville, FL 32611-6580, USA

(Received April 13, 2010, Accepted May 31, 2011)

Abstract. This paper is focused on the residual capacity of steel columns, as a damage criterion. Load-Impulse (P-I) diagrams are frequently used for analysis, design, or assessment of blast resistant structures. The residual load carrying capacity of a simply supported steel column was derived as a damage criterion based on a SDOF computational approach. Dimensionless P-I diagrams were generated numerically with this quantitative damage criterion. These numerical P-I diagrams were used to show that traditional constant ductility ratios adopted as damage criteria are not appropriate for either the design or damage assessment of blast resistant steel columns, and that the current approach could be a much more appropriate alternative.

Keywords: residual load carrying capacity; blast; steel column; P-I diagram

1. Introduction

Blast resistant buildings should be designed to protect occupants and equipments by limiting structural damage to within an acceptable range. Structural engineers are concerned with preventing localized blast-induced damage from evolving into a global building failure. Bomb damage assessment (BDA) is based on the ratio of collapsed floor slab area to total building area (Morris 2004). When this ratio is between 75% and 100%, the building is considered as “Destroyed”, while it is assumed to be “Severely Damaged” for a damage ratio between 45% and 75% (DIA 2003). A current guide for preventing progressive collapse (Department of Defense 2009) recommends limiting the collapsed floor area directly above a removed column to be less than the smaller of either 70 m^2 or 15% of that floor area. These two examples show that the collapsed or failed area has been adopted as a parameter to express the severity of building damage, and they are directly related to the failure of a supporting column.

The potential for global building damage must be based on assessing local damage of critical structural components, such as a column or a load bearing wall. Load-Impulse diagrams are a form of a shock response spectrum, and they have been widely used for damage assessment of structural

*Corresponding author, Senior Researcher, E-mail: jongyilpark@gmail.com
[a]Goldsby Professor

elements (Krauthammer 2008, Krauthammer *et al.* 2008, Soh and Krauthammer 2004). The load can be in the form of peak force or peak pressure, while the impulse is the area under the load-time history. P-I diagrams represents combinations of peak load and corresponding impulse that cause a predetermined level of structural response (e.g., cracking, yielding, fracture, a specific displacement, etc.). P-I diagrams can be utilized as standardized failure criteria of all structure components in computer based building damage analysis tools.

A P-I diagram divides the load vs. impulse space into two distinct regions. Load-impulse combinations falling to the left or below the P-I curve cannot cause the predetermined level of structural response, while those to the right and above the curve produce structural response exceeding the predetermined response level. The structural dynamic response has a strong relationship with the natural frequency of structural element and the duration of load function, which can be categorized into three regions; the impulsive, quasi-static and dynamic domains, as shown in Fig. 1 (Krauthammer 2008, Krauthammer *et al.* 2008). In the impulsive loading region, the pressure duration is very short relative to the response time of the structure. Since the pressure is quickly removed before any significant structural deformation, the maximum structural response can be assumed to depend on the applied impulse and not on the form of the pressure-time history. In the quasi-static region, the pressure duration is significantly longer than the structural response time. Since the applied pressure dissipates very little before the maximum deflection occurs (i.e., almost constant pressure acts while deflection occurs), the structural response depends only upon the peak pressure. As with the impulsive region, the maximum response in this region may not dependent on the entire pressure-time history. The dynamic domain exists between the impulsive and quasi-static regions, where the pressure duration and the system response time are of the same order. The structural response in this region depends on the pressure-time history. For BDA or preliminary protective design, the asymptote equations for the impulsive and quasi-static domains

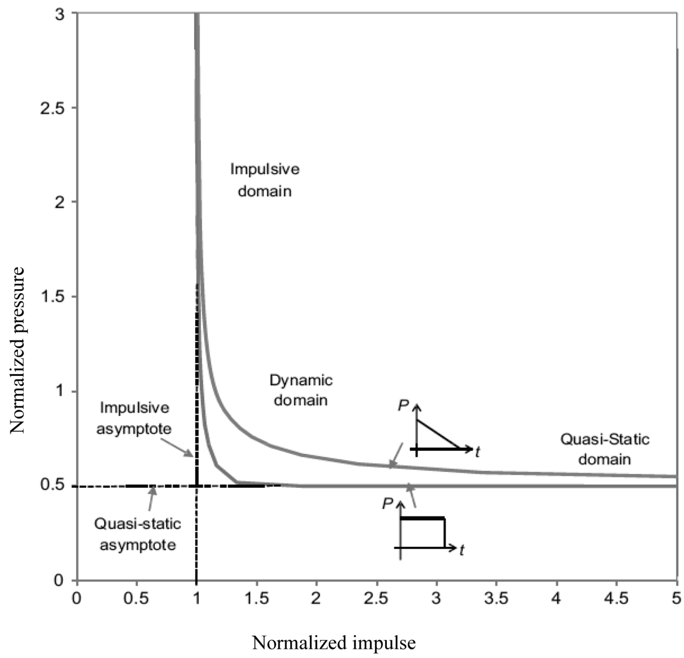

Fig. 1 Characteristics of P-I diagrams (Krauthammer *et al.* 2008)

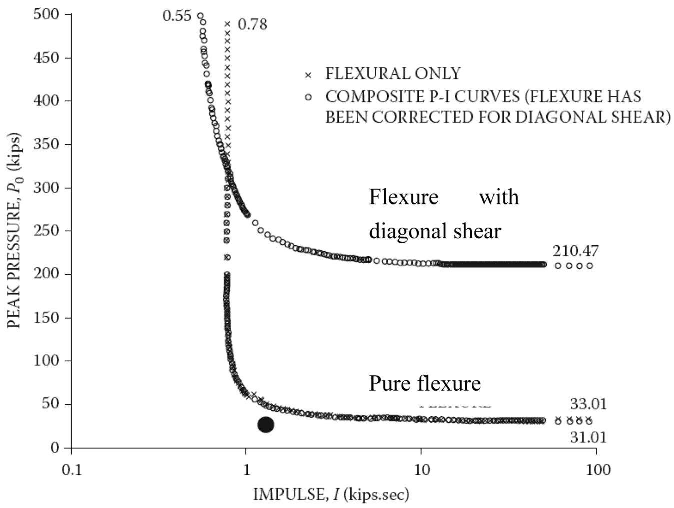

Fig. 2 P-I diagrams for flexure and direct shear (Soh and Krauthammer 2004)

can be utilized to determine the component status after explosive loading with simple and quick calculations (Krauthammer 2008, Krauthammer *et al.* 2008). The short calculation time from the asymptote concept, which needs only applied impulse value, could be essential especially in emergency situation, where the expected damage of targets or BDA analysis must be completed within very short times, without performing complete time history analyses or with the complete P-I curve.

Flexure and direct shear responses are expected in structural components under severe blast loading (Krauthammer 2008). Since these two failure mechanisms do not occur simultaneously, two loosely coupled equivalent Single Degree of Freedom (SDOF) systems can be adopted to generate P-I diagrams (Soh and Krauthammer 2004). One should note that the flexural P-I curve can be modified to include the effects of diagonal shear, and/or axial loads. This can be done by overlaying a P-I curve for direct shear response to the one for flexural response, as shown in Fig. 2. Thus, it is appropriate to develop a P-I diagram for each response mode independently, and to overlay the resulted P-I curves on the same graph to obtain a final damage assessment curve.

Typically, P-I diagrams have been generated by adopting a SDOF model, which consists of a mass, and a resistance for an assumed structural component mode shape (Krauthammer 2008, Krauthammer *et al.* 2008). In this study, the focus is on developing an appropriate approach for the damage assessment of steel columns by using the P-I concept and well founded theoretical and behavioral models. For flexural response of column under lateral loading at midspan, the following SDOF governing equation can be derived

$$K_{LM}M\ddot{u}(t) + R(u(t)) = F(u(t), t) \tag{1}$$

where $u(t)$ is the column midspan deflection, M is the total column mass, $R(u(t))$ is the column lateral resistance function, $F(u(t), t)$ is the applied force, and K_{LM} is the load-mass factor of a column under lateral concentrated loading at midspan, which is 0.49 (elastic deformation), 0.33 (inelastic deformation) for simply supported boundary condition (Bigg 1964). K_{LM} depends on the mode shape assumption, which induces the same energy distribution as that of the real distributed mass. For direct shear without damping, the equivalent SDOF model can be given as the following (Krauthammer *et al.* 1990)

$$M_s\ddot{y}(t) + R_s = V(t) \tag{2}$$

where y is the direct shear slip, M_s is the equivalent shear mass, R_s is the dynamic resistance function for direct shear, $V(t)$ is the dynamic reaction.

It is common to use the maximum ductility ratio, μ, and support rotation, θ, as damage criteria for P-I curves, as shown in Tables 1 and 2 (US Army 2006). For example, a compact steel column is considered to suffer "Heavy Damage" when the maximum ductility ratio is larger than 3, or the maximum rotation is larger than 3°. However, the response limits in Table 2 cannot be utilized directly in the global damage analysis, although damage levels are described in Table 1. To derive the global damage, it is necessary to obtain quantitative damage values for critical structural components. For columns, the residual axial load carrying capacity, after a blast loading incident, could be an important damage criterion for assessing secondary damage and the potential for progressive collapse. Few researches studied the residual load carrying capacity of a column after blast events. Bao and Li (2010) and Shi *et al.* (2007) obtained P-I diagrams based on residual load carrying capacity by adopting finite element analyses with LS-DYNA (LS-DYNA 2006). However,

Table 1 Description and corresponding response limits (US Army 2006)

Component Damage Level	Description of Component Damage	Relationship to Response Limits (Table 2)
Blowout	Component is overwhelmed by the blast load causing debris with significant velocities	Response greater than B4.
Hazardous Failure	Component has failed, and debris velocities range from insignificant to very significant	Response between B3 and B4.
Heavy Damage	Component has not failed, but it has significant permanent deflections causing it to be unrepairable	Response between B2 and B3.
Moderate Damage	Component has some permanent deflection. It is generally repairable, if necessary, although replacement may be more economical and aesthetic	Response between B1 and B2.
Superficial Damage	Component has no visible permanent damage	Response is less than B1.

Table 2 Response Limits for Hot Rolled Structural Steel (US Army 2006)

Member		B1		B2		B3		B4	
		μ	θ	μ	θ	μ	θ	μ	θ
Flexure	Compact or seismic member	1		3	3°	12	10°	25	20°
	Non compact member	0.7		0.85		1.0		1.2	
	Plate	4	1°	8	2°	20	6°	40	12°
Combined Flexure & Compression	Compact or seismic member	1		3	3°	3	3°	3	3 °
	Non compact member	0.7		0.85		0.85		0.85	
Compression		0.9		1.3		2		3	

theoretical analysis methods to generate P-I curves were not presented, which could be essential to show the interactions of numerous parameters (such as component geometry, material, axial loading condition, damage level etc.) systematically. Furthermore, expedient blast damage assessment cannot be handled with fully nonlinear dynamic finite element simulations, and one needs a much faster approach, such as with a well-formulated SDOF system.

In this paper, a new methodology to generate P-I diagrams for steel columns is proposed, based on the flexural SDOF model and residual axial load carrying capacity of a steel column. This type of P-I diagram can be adopted to obtain a safety factor for the local column response after an abnormal loading dissipates, and to conduct accurate secondary damage analysis for building systems. Corresponding theoretical asymptote equations are proposed, based on adopting the energy balance method, which can be adopted in preliminary protective design and for urgent analyses during emergency operations, without generating whole P-I curves. Also, the validity of a constant ductility limit in Table 2, as a damage criterion, is checked.

2. SDOF model for simply supported column under blast loading

Fig. 3 shows a building face subjected to an explosive loading. The structural system for that face consists of four beams and three columns with span lengths L_b and L_c, respectively. When the columns are simply supported, and beam-column connections are assumed to be hinges, an equivalent flexural SDOF model for a middle column can be expressed by Eq. (1). The lateral resistance function R is assumed as elastic-perfectly plastic, as shown in Fig. 4, and the elastic stiffness of the resistance function has the same form as the one for beams (US Army 1986)

$$K_c = \frac{48EI}{L_c^3} \tag{3}$$

where E is Young's modulus of elasticity, L_c is the column length, and I is the second moment of area.

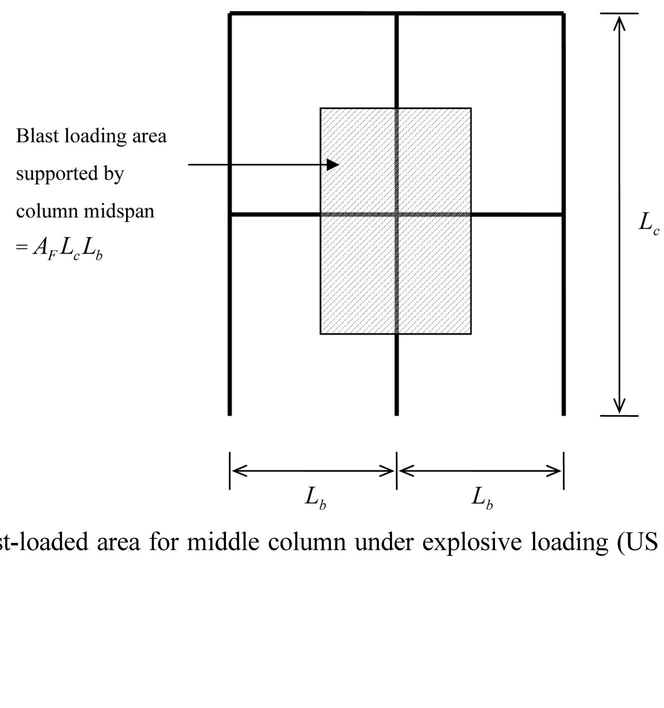

Fig. 3 Blast-loaded area for middle column under explosive loading (US Army 2006)

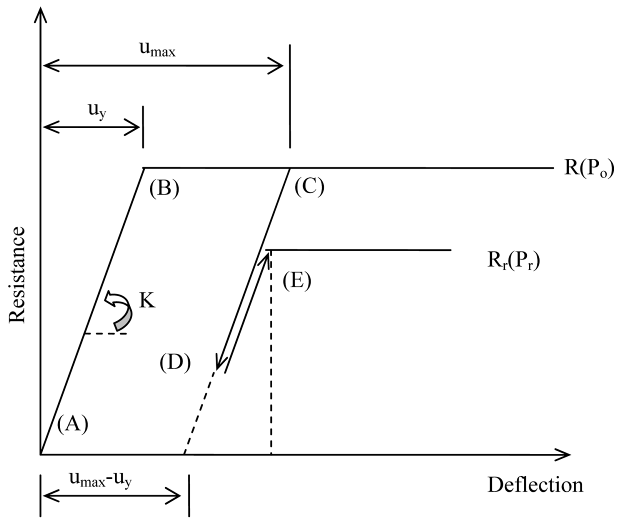

Fig. 4 Resistance function

Since a column is loaded to a constant axial force P_0, the neutral axis does not coincide with the centroid at the maximum value of the resistance function. Thus, the maximum resistance R_y and corresponding deflection u_y should be defined as follows

$$R_y = \frac{4M_p}{L_c} \tag{4}$$

$$u_y = \frac{R_y}{K} \tag{5}$$

where M_p is the plastic moment of the cross section

$$M_p = Zf_y(1-\alpha^2) \tag{6}$$

$$P_o = \alpha f_y A \tag{7}$$

where Z is the plastic section modulus, A is the cross section area, f_y is the yield stress of steel, and α is the axial load ratio.

For columns under blast loading, the P-delta effect from a constant axial force P_0 and the midspan deflection $u(t)$ should be considered, as shown in Fig. 5. The P-delta effect can be accounted for by adopting the equivalent lateral load, which acts in addition to the existing lateral load to cause the same midspan moment. This additional equivalent lateral load, F_e, can be expressed by (US Army 2006, Timoshenko and Gere 2009)

$$F_e(t) = \frac{4P_0u(t)}{L_c} \tag{8}$$

Thus, the total applied lateral load $F(t)$ in Eq. (1) can be formulated as

$$F(t) = F_1(t) + F_e(t) \tag{9}$$

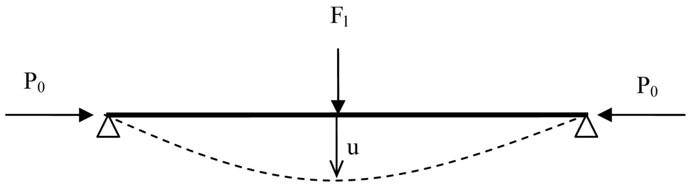

Fig. 5 P-delta effect for column

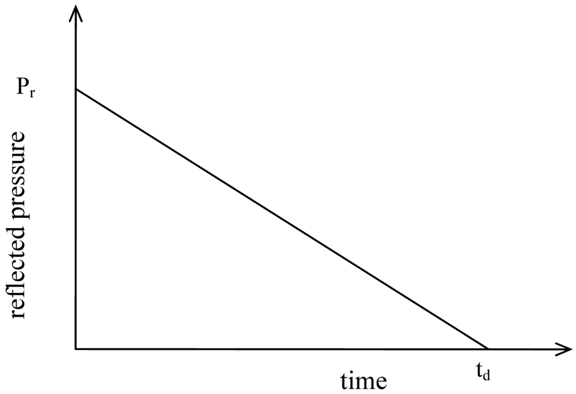

Fig. 6 Simplified triangular reflected pressure history

where F_1 is the lateral explosion load, assuming that the reflected pressure history is a right triangular shape, as shown in Fig. 6, and can be expressed by

$$F_1(t) = F_{\max}[1 - t/t_d] \quad \text{when} \quad t \le t_d$$

$$F_1(t) = 0 \quad \text{otherwise} \tag{10}$$

Where

$$F_{\max} = P_r L_b L_c A_F \tag{11}$$

$$t_d = 2I_r/P_r \tag{12}$$

and P_r is the peak reflected pressure, L_b is the beam length, I_r is the reflected pressure impulse, t_d is the reflected pressure duration, and A_f is the load area factor that represents the blast loading area supported by the column midspan, as shown in Fig. 3 (US Army 2006).

3. Residual axial load carrying capacity

The midspan deflection history can be obtained by solving Eq. (1) numerically. If the resistance function reaches the yield point, such as the path through (A)→(B)→(C) in Fig. 4, there will be a residual deflection at point (D). It should be noted that the axial force remains constant in the path through (A)→(B)→(C)→(D). The residual axial load carrying capacity, which represents the axial load carrying capacity of the damaged column after blast event, can be determined by increasing the applied axial load moving up the resistance function graph from point (D) to (E). Since the maximum resistance depends on the applied axial load, as shown in Eqs. (4) and (6), the load magnitudes at points (C) and (E) are different. When the residual load carrying capacity is P_{lc}, the maximum resistance R_r can be derived from Eqs. (4) and (6), as follows

$$R_r = \frac{4Zf_y}{L_c}(1-\beta^2) \tag{13}$$

where β is the residual load carrying capacity ratio, which satisfies $P_{lc} = \beta f_y A$.

At point (E), the static P-delta equilibrium should be satisfied by Eq. (8), as follows

$$R_r = \frac{4P_{lc}(u_{\max}-u_y+R_r/K)}{L_c} \tag{14}$$

where u_y is the yield deflection when the axial load is P_0, and $u_{\max}$ is the maximum deflection in Fig. 4.

By combining Eqs. (13) and (14), the maximum ductility ratio μ (which is $u_{\max}/u_y$), related to the residual load carrying capacity ratio β, can be determined by

$$\mu = 1+\frac{(1-\beta^2)}{(1-\alpha^2)}\left(\frac{1}{4\beta}\frac{KL_c}{F_y}-1\right) \tag{15}$$

where F_y is the yield force for the column cross section, which is f_yA.

4. Generation of P-I diagrams

4.1 Asymptote equations based on energy balance method

The energy balance method, as described in Krauthammer (2008), can be adopted to calculate the impulsive and quasi-static asymptotes for P-I diagrams (Fig. 1). The following simple expressions are used for asymptotes calculation (Krauthammer 2008)

$$\text{K.E.} = \text{S.E.} \quad \text{(for the impulsive asymptote)} \tag{16}$$

$$\text{W.E.} = \text{S.E} \quad \text{(for the quasi-static asymptote)} \tag{17}$$

where, K.E. is the kinetic energy acquired by the column at time zero, W.E. is the work done by the applied force from time zero to the maximum deflection, S.E. is the strain energy at the maximum deflection. The energy terms for an axially-loaded column under lateral blast loading are given by the following expressions

$$\text{K.E.} = \frac{I_F^2}{2K_{LM}M} \tag{18}$$

$$\text{W.E.} = F_{\max}u_{\max}+\frac{2P_0}{L_c}u_{\max}^2 \tag{19}$$

$$\text{S.E.} = Ku_y^2\left(\mu-\frac{1}{2}\right) \tag{20}$$

where I_F is the impulse (the area under the force vs. time function, in units of force multiplied by time), which is $I_r L_b L_c A_F$ from Eqs. (11) and (12).

From Eqs. (16), (18), and (20), the impulsive asymptote can be expressed by the following dimensionless equation

$$\frac{I_F}{\sqrt{K_{LM} M K u_y}} = \sqrt{2\mu - 1} \tag{21}$$

From Eqs. (17), (19), and (20), the quasi-static asymptote can be derived, as follows

$$\frac{F_{\max}}{K u_y} = \left(\frac{2\mu - 1}{2\mu}\right) - 2\mu\alpha\left(\frac{F_y}{KL}\right) \tag{22}$$

It can be seen from Eqs. (15), (21), and (22) that the dimensionless asymptotes can be expressed by the initial axial load ratio, α, the desired residual load carrying capacity ratio, β, and the column property KL_c/F_y.

Due to the P-delta effect from a constant axial force P_0, the column may become unstable at a certain deflection. When the deflection reaches a maximum value $u_{\max}$ at time $t_{\max}$, the velocity $\dot{u}|_{t_{\max}}$ should be zero, and the acceleration $\ddot{u}|_{t_{\max}}$ should be negative. Since in the impulsive domain, the duration of a blast load is much shorter than $t_{\max}$ the governing equation after $t_{\max}$ can be expressed by Eq. (1) as follows

$$K_{LM} M \ddot{u}_a + R_y + K u_a = \frac{4\alpha F_y}{L_c}(u_{\max} + u_a) \tag{23}$$

where u_a is the deflection reached after $t_{\max}$, which satisfies $u = u_{\max} + u_a$.

With Eq. (23) and the initial conditions: $u_a|_{t_{\max}} = 0, \dot{u}_a|_{t_{\max}} = 0, \ddot{u}_a|_{t_{\max}} < 0$, the following relationship should be satisfied

$$\mu \leq \frac{KL_c}{4\alpha F_y} \tag{24}$$

Eq. (24) represents the limit of a possible maximum ductility ratio for the impulsive asymptote. If the ductility ratio for a given residual load carrying capacity ratio from Eq. (15) violates Eq. (24), the column is unstable. That is, the given residual load carrying capacity ratio does not satisfy the requirement associated with the impulsive asymptote.

For the quasi-static asymptote, the governing equation after $t_{\max}$ can be expressed, as follows

$$K_{LM} M \ddot{u}_a + R_y + K u_a = \frac{4\alpha F_y}{L_c}(u_{\max} + u_a) + F_{\max} \tag{25}$$

Similarly to the impulsive asymptote case, the ductility ratio limit is given by the following expression

$$\mu \leq \frac{(K - F_{\max}/u_y) L_c}{4\alpha F_y} \tag{26}$$

4.2 Numerical approach

P-I diagrams can be generated by computing sufficient data points with the SDOF approach that represent pressure and impulse combinations satisfying predetermined damage values (e.g., a given strain, deflection, etc.). Since two asymptotes exist for the P-I curve, both need to be computed. For the impulsive region, data points are generated with fixed pressure values while increasing the impulse. For the quasi-state region, the data points are generated with fixed impulse values while increasing the pressure. Any of these two processes can be used for the dynamic region. However, the separate analyses approach for the three P-I diagram regions requires the definition of boundaries of these regions before starting the analyses. Alternatively, the innovative approach proposed in Krauthammer *et al.* (2008) can be used to address all three regions in a single computational sweep.

In this paper, it is proposed to generate P-I diagrams by using Charge Weight Standoff (CWSD) diagrams, which correspond directly to specific lod-time histories that define combinations of peak load and total impulse. However, since load and impulse combinations correspond to specific structural response values, the same CWSD diagrams would correspond to predetermined response limits. Since larger amounts of TNT are required to cause a predetermined damage state, as the standoff distance increases, the corresponding pressure and impulse data points can be obtained without boundary definitions by trial and error searches with CWSD diagrams.

To illustrate this approach, P-I diagrams for a simply supported W 690×265 steel column were generated based on the residual load carrying capacity approach. The solution of Eq. (1) was obtained numerically by using MATLAB, and the central difference method (Rao 1995). Table 3 summarizes the properties of the analyzed column. The geometry of the analyzed frame is shown in Fig. 3, where the column and beams lengths were assumed as 10 m and 5 m, respectively.

Table 3 Material and column section properties

Material		Column (W690 × 265)	
E	200 GPa	I	0.0029 m^4
f_y	345 MPa	d	706 mm
		A	0.033 mm^2
		Z	0.00929 m^3

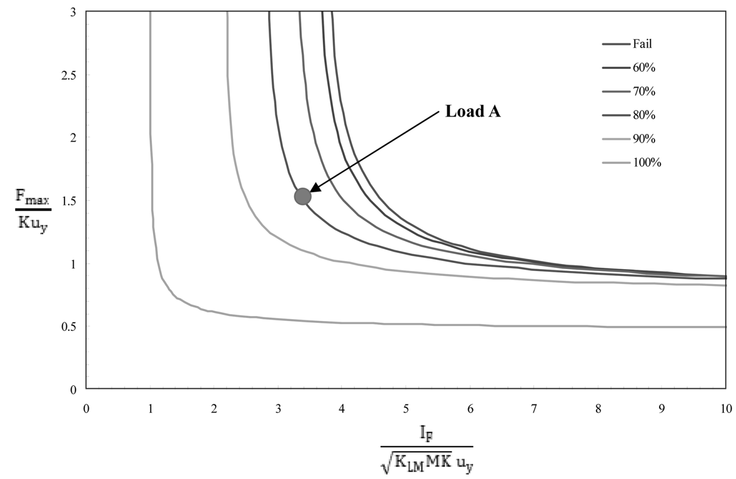

Fig. 7 P-I Diagrams for $\alpha = 0.5$

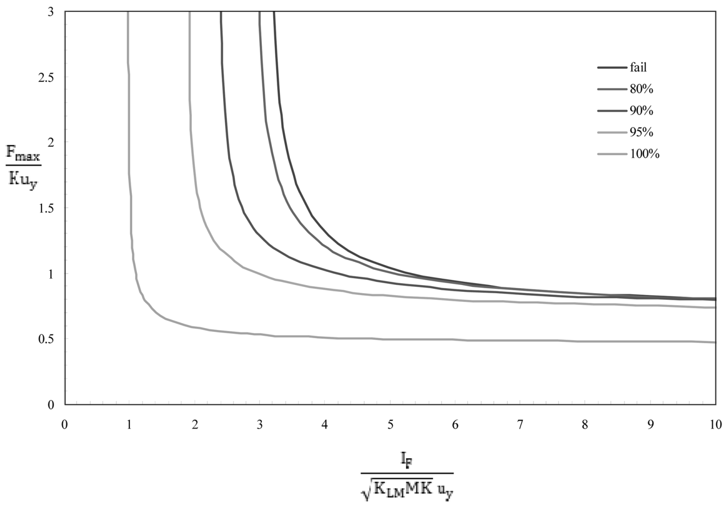

Fig. 8 P-I Diagrams for $\alpha = 0.7$

The load area factor A_F was assumed as 0.5. Figs. 7 and 8 show the P-I diagrams for the column under two different initial axial load ratios ($\alpha = 0.5$ and 0.7), for which safety factors before blast loading can be determined as 2 and 1.43 (=1/α), respectively. The legends of the curves in Figs. 7 and 8 represent the residual load carrying capacity ratio, β as a percentage, showing that the column can support the axial force βF_y after the blast load dissipates. The "fail" condition is a load combination under which the column is unstable, and buckling occurs. The corresponding safety factors after blast loading can be defined as β/α, as shown in Table 4. For example, when a column under a constant axial load of 5.8 MN ($\alpha = 0.5$) is subjected to load A in Fig. 7, the residual load carrying capacity ratio is 0.80. That is, the column can endure an axial load of 9.3 MN after the blast loading event, corresponding to a safety factor of 1.6, as shown in Table 4.

In Figs. 7 and 8, some of the P-I diagrams seem to converge to the "fail" P-I curves in the high impulsive regions. This can be explained by Eq. (26). Tables 5 and 6 show the required ductility for a given residual load carrying capacity ratio from Eq. (15), the ductility limits for the impulsive asymptote from Eq. (24) and for the quasi-static asymptote from Eq. (26). The shaded area in Tables 5 and 6 show where the required ductility exceeds the ductility limit. For the case of $\alpha = 0.5$,

Table 4 Safety factors

Residual Axial Load Carrying Capacity Ratio*100 100β	Safety Factors (β/α)	
	when $\alpha = 0.5$	when $\alpha = 0.7$
100%	2.00	1.43
95%	1.90	1.36
90%	1.80	1.29
85%	1.70	1.21
80%	1.60	1.14
75%	1.5	1.07
Fail	0	0

Table 5 Ductility Limits for $\alpha = 0.5$

Residual Load Carrying Capacity Ratio β	Ductility Ratio μ [Eq. (15)]	Impulsive Asymptote		Quasi-Static Asymptote	
		$\frac{I_F}{\sqrt{K_{LM}MKu_y}}$	Ductility Limit [Eq. (24)]	$\frac{F_{max}}{Ku_y}$	Ductility Limit [Eq. (26)]
0.60	8.69	4.05	12.01	0.58	5.04
0.64	7.60	3.77	12.01	0.62	4.59
0.68	6.61	3.50	12.01	0.65	4.22
0.72	5.71	3.23	12.01	0.67	3.91
0.76	4.89	2.96	12.01	0.69	3.67
0.80	4.12	2.69	12.01	0.71	3.52
0.84	3.41	2.41	12.01	0.71	3.47
0.88	2.75	2.12	12.01	0.70	3.56
0.92	2.13	1.81	12.01	0.68	3.88
0.96	1.55	1.45	12.01	0.61	4.65
1.00	1.00	1.00	12.01	0.46	6.51

Table 6 Ductility limits for $\alpha = 0.7$

Residual Load Carrying Capacity Ratio β	Ductility Ratio μ [Eq. (15)]	Impulsive Asymptote		Quasi-Static Asymptote	
		$\frac{I_F}{\sqrt{K_{LM}MKu_y}}$	Ductility Limit [Eq. (24)]	$\frac{F_{max}}{Ku_y}$	Ductility Limit [Eq. (26)]
0.82	5.06	3.02	8.58	0.61	3.38
0.84	4.55	2.85	8.58	0.62	3.22
0.86	4.06	2.67	8.58	0.64	3.09
0.88	3.58	2.48	8.58	0.65	2.99
0.90	3.11	2.29	8.58	0.66	2.93
0.92	2.66	2.08	8.58	0.66	2.94
0.94	2.23	1.86	8.58	0.65	3.04
0.96	1.81	1.62	8.58	0.62	3.28
0.98	1.40	1.34	8.58	0.56	3.77
1.00	1.00	1.00	8.58	0.44	4.79

the required ductility ratios are larger than the ductility limits when the residual load carrying capacity ratio is less than 0.80 for the quasi-static asymptote. That means that the quasi-static asymptote for less than about 0.80 residual load carrying capacity ratios coincides with the quasi-static asymptote for failure. For the case of $\alpha = 0.7$, this condition occurs when β is less than about 0.9. It should be noted that the required ductility ratios are not a constant value in Tables 5 and 6. Even if the required residual load carrying capacity is a constant value, the required ductility ratio calculated from Eq. (15) depends on the initial axial load ratio, α, and the column property, KL_c/F_y. Thus, the constant ductility criterion from PDC-TR 06-08 (2006) may not be appropriate for damage assessment of columns. The present approach seems to be a more appropriate alternative that is well founded on basic structural mechanics and dynamic principles.

5. Conclusions

The residual strength of a column is essential for evaluating post-incident global building safety. A theoretical method was proposed for obtaining dimensionless P-I diagrams, based on the residual load carrying capacity of simply supported steel columns with constant axial loads after blast loading events. That residual load carrying capacity was derived with a SDOF approach and elastic perfectly-plastic resistance functions, and P-Δ effects. Consequently, this approach can easily be implemented to any structural element that can be defined by a combination of general material and geometric nonlinear resistance functions.

For urgent situations and preliminary design stages, impulsive and quasi-static asymptote equations were derived by adopting the energy balance method. Since the only input parameters needed for obtaining the proposed dimensionless asymptotes are the initial axial load ratio, α, the desired residual load carrying capacity ratio, β, and the column property, KL_c/F_y, the proposed approach can be easily implemented in existing computer-based building damage analysis tools. This modification is expected to significantly enhance the accuracy of global building damage analyses without increasing calculation times and/or computational resources.

A theoretical relationship was derived for the ductility ratio and the residual load carrying capacity ratio (Eq. (15)). Based on this equation and the obtained P-I diagrams, it is noted that a constant ductility ratio is not appropriate as a damage criterion for extreme dynamic loading events, especially for global building stability analysis, such as trigger for progressive collapse.

Although the direct shear at supports could be a failure mechanism at certain pressure-impulse domain levels, P-I curves from direct shear and flexure can be independently prepared and combined with the flexural P-I curves, as noted earlier. Moreover, the residual load carrying capacity concept is not appropriate in direct shear based P-I diagram since the direct shear failure is considered as a brittle structural response.

References

Bao, X. and Li, B. (2010), "Residual strength of blast damaged reinforced concrete columns", *Int. J. Impact Eng.*, **37**.

Biggs, J.M. (1964), *Introduction to Structural Dynamics*, McGraw-Hill.

Defense Intelligence Agency (2003), DI-2820-4-03: BDA Quick Guide, Department of Defense Intelligence Production Program.

Department of Defense (2009), UFC 4-023-03: Design of Building to Resist Progressive Collapse, US Army Corps of Engineers, 14 July.

Krauthammer, T. (2008), *Modern Protective Structures*, CRC Press.

Krauthammer, T., Astarlioglu, S. and Blasko, J.R. (2008), "Pressure-impulse diagrams for the behavior assessment of structural components", *Int. J. Impact Eng.*, **35**(8), 771-783.

Krauthammer, T., Shahriar, S. and Shanaa, H.M. (1990), "Response of RC elements to severe impulsive loads", *J. Struct. Eng.*, **116**.

LS-DYNA Keyword User's Manual (2006), Livermore Software Technology Coporation.

Morris, D. (2004), "Weaponeering: conventional weapon system effectiveness", AIAA Educational Series, AIAA Inc.

Rao, S.S. (1995), *Mechanical Vibrations*, Addison-Wesley.

Shi, Y., Hao, H. and Li, Z.X. (2007), "Numerical derivation of pressure-impulse diagrams for prediction of RC column damage to blast loads", *Int. J. Impact Eng.*, **35**.

Soh, T.B. and Krauthammer, T. (2004), “Load-impulse diagrams of reinforced concrete beams subjected to concentrated transient loading”, Final Report to U.S. Army, ERDC, PTC–TR-006-2004, Protective Technology Center, Pennsylvania State University, April.

Timoshenko, S.P. and Gere, J. (2009), *Theory of Elastic Stability*, Dover Publications.

US Army (2006), PDC-TR 06-01: Methodology Manual for the Single-Degree-of-Freedom Blast Effects Design Spreadsheets, US Army Corps of Engineers.

US Army (2006), PDC-TR 06-08: Single Degree of Freedom Structural Response Limits for Antiterrorism Design, US Army Corps of Engineers.

US Army (1986), TM 5-855-1: Fundamentals of Protective Design for Conventional Weapons, US Army Waterways Experimental Station.

Notations

α : initial axial load ratio
β : residual load carrying capacity ratio
μ : ductility ratio
θ : slope
A : cross section area
A_F : load area factor
d : section depth
E : Young's modulus of elasticity of steel
F : applied force in SDOF model
F_e : equivalent lateral load by P-delta effect
F_l : lateral load by explosion
F_y : yield force of column cross section, which is f_yA
f_y : yield stress of steel
I : second moment of area
I_F : impulse (force multiplied by time)
I_r : impulse of reflected pressure
K : elastic stiffness of resistance
K_{LM} : load mass factor
L_b : beam span length
L_c : column span length
M : total mass of column
M_p : plastic moment
M_s : equivalent shear mass
P_{lc} : residual load carrying capacity
P_0 : initial axial load
P_r : reflected peak pressure
$R(u(t))$: lateral resistance function of column
R_s : dynamic resistance function for direct shear
R_y : yield resistance
t_d : duration of reflected pressure
$u(t)$: column midspan deflection
$u_{\max}$: maximum deflection
u_y : yield deflection
$V(t)$: dynamic reaction.
y : direct shear slip
Z : plastic section modulus